



Chemical and strontium isotopic characteristics of shallow groundwater in the Ordos Desert Plateau, North China: Implications for the dissolved Sr source and water–rock interactions

Wenbo Rao ^{a,*}, Ke Jin ^a, Sanyuan Jiang ^b, Hongbing Tan ^a, Liangfeng Han ^c, Quanyong Tang ^d



^a Institute of Isotope Hydrology, College of Earth Sciences and Engineering, Hohai University, Nanjing 210098, China

^b State Key Laboratory of Lake Science and Environment, Nanjing Institute of Geography and Limnology, Chinese Academy of Sciences, Nanjing 210008, China

^c Isotope Hydrology Section, Division of Physical and Chemical Sciences, Department of Nuclear Sciences and Applications, International Atomic Energy Agency, P.O. Box 100, A-1400 Vienna, Austria

^d Xiaolangdi Dam Project and Management Bureau, The Ministry of Water Resources of China, Zhengzhou 450000, China

ARTICLE INFO

Article history:

Received 22 September 2014

Received in revised form 16 April 2015

Accepted 8 July 2015

Editorial handling - H. Guo

Keywords:

Sr isotopic composition

Groundwater system (GWS)

Dissolved Sr source

Water–rock interaction

Ordos Desert Plateau

ABSTRACT

In this study, the chemical and Sr isotopic compositions of shallow groundwater and rainwater in the Ordos Desert Plateau, North China, and river water from the nearby Yellow River, are investigated to determine the dissolved Sr source and water–rock interactions, and quantify the relative Sr contribution from each end-member. Three groundwater systems have been identified, namely, GWS-1, GWS-2 and GWS-3 according to the watershed distribution in the Ordos Desert Plateau. Ca^{2+} and Mg^{2+} are the most dominant cations in GWS-1, while Na^+ is dominant in GWS-3. In addition, there is more SO_4^{2-} and less Cl^- in GWS-1 than in GWS-3. The shallow groundwater in GWS-2 seems to be geochemically between that in GWS-1 and GWS-3. The $^{87}\text{Sr}/^{86}\text{Sr}$ ratios of the shallow groundwater are high in GWS-1 and GWS-2 and are low in GWS-3. By geochemically comparing the nearby Yellow River, local precipitation and deep groundwater, the shallow groundwater is recharged only by local precipitation. The ionic and isotopic ratios indicate that carbonate dissolution is an important process controlling the chemistry of the shallow groundwater. The intensity of the water–rock interactions varies among the three groundwater systems and even within each groundwater system. Three end-members controlling the groundwater chemistry are isotopically identified: (1) precipitation infiltration, (2) carbonate dissolution and (3) silicate weathering. The relative Sr contributions of the three end-members show that precipitation infiltration and carbonate dissolution are the primary sources of the shallow groundwater Sr in GWS-3 whereas only carbonate dissolution is responsible for the shallow groundwater Sr in GWS-1 and GWS-2. Silicate weathering seems insignificant towards the shallow groundwater's chemistry in the Ordos Desert Plateau. This study is helpful for understanding groundwater chemistry and managing water resources.

© 2015 Elsevier GmbH. All rights reserved.

1. Introduction

The arid and semi-arid area in North China is large, covering >100 million km² (Zhu et al., 1980). Due to rare rainfall and strong evaporation, shallow groundwater is an important component of water resources to feed local people, maintain plant growth and prevent soil desertification in this area (Yang et al., 2004). In addition, the groundwater level is declining and the eco-environment is worsening as aridification is strengthening and human activities

increase (Feng et al., 2000). Therefore, it is necessary to understand the evolution and origin of the shallow groundwater's chemistry for the sustainable utilization of the regional-scale water resources in the arid and semiarid area of China.

Sr isotopes can be used as a good tool for tracing the evolution and origin of groundwater chemistry. Authors have demonstrated the advantage of Sr isotopes as tracers in hydrogeological studies (Woods et al., 2000; Négrel et al., 2001, 2003, 2004; Harrington and Herczeg, 2003; Gosselin et al., 2004; Frost and Toner, 2004; de Caritat et al., 2005; Wang et al., 2006; Petelet-Giraud et al., 2007; Cartwright et al., 2007; Raiber et al., 2009). For example, Négrel et al. (2004) coupled Sr isotopic and chemical compositions to trace riverbank aquifer recharge and chemical transfer between surface

* Corresponding author.

E-mail address: raowenbo@163.com (W. Rao).

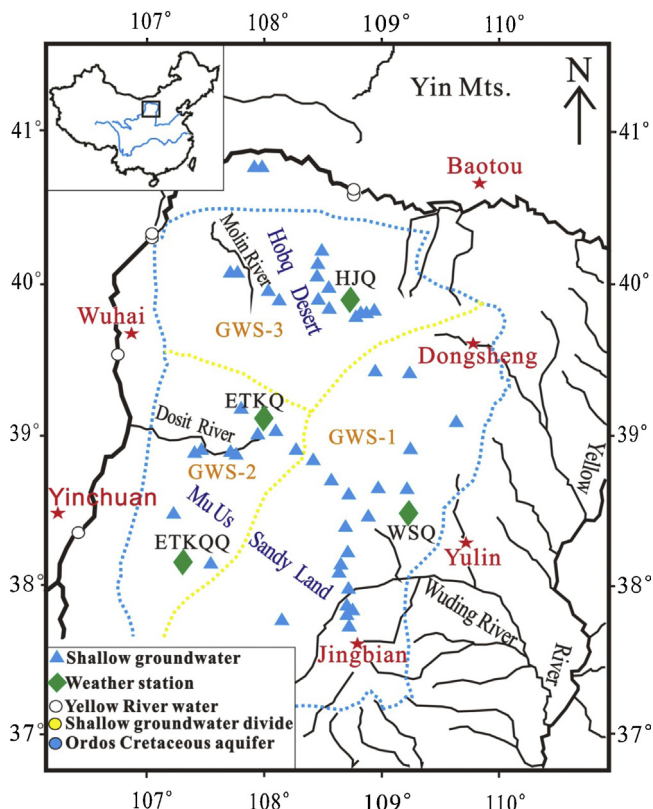


Fig. 1. Map showing the study area and sampling locations.

and ground water; Wang et al. (2006) used Sr isotopes and major ions to identify the flow paths of karst water and hydrochemical processes in the Shentou karst system of northern China; and Raiber et al. (2009) revealed the recharge and salinization mechanisms of groundwater in the basalt plains of southeastern Australia by using Sr isotopes. The successful use of Sr isotopes is ascribed to the following reasons: (1) different aquifer rocks have different $^{87}\text{Sr}/^{86}\text{Sr}$ ratios due to their different Rb/Sr ratios and ages, so the groundwater $^{87}\text{Sr}/^{86}\text{Sr}$ ratios may reflect the contribution of aquifer rock weathering and water recharge (Faure, 1991; McNutt, 2000); (2) ^{87}Rb decay has a negligible effect on the $^{87}\text{Sr}/^{86}\text{Sr}$ ratio of groundwater with a residence time <1 Ma due to its long half-life (48.8×10^9 a) (Kossert, 2003); and (3) Sr isotopes are not fractionated appreciably in nature during surficial processes (Capo et al., 1998; Shand et al., 2009). However, Sr isotopes have rarely been used as tracers to delineate the geochemical evolution and origin of groundwater in the arid and semiarid area of North China (Wang et al., 2006; Xie et al., 2013).

In this study, the study area of interest is the Ordos Desert Plateau. The Ordos Desert Plateau is situated in the middle of the Yellow River drainage and is an important component of the arid and semiarid area in North China (Fig. 1). In this plateau, sandstorms happen frequently and there are plenty of mineral resources such as metals, coal and oil (Li et al., 2007b; Hou et al., 2004; Wang et al., 2004). In recent years, the pressure between the supply and demand of water resources went up rapidly with the exploitation of mineral resources, the increasing number of various factories and the improvement of people's living standard. To relieve this pressure, some studies have been conducted on the groundwater in the Ordos Desert Plateau. For example, Hou et al. (2008) systematically described the classification and flow pattern of groundwater from a hydrogeological perspective; Yin et al. (2010, 2011a) argued that the groundwater is of meteoric origin through a D-O isotopic comparison of the groundwater with other waters; Yin et al. (2011b)

estimated recharge mechanism of the groundwater by using multiple methods such as water table fluctuation, Darcy's law and the water budget; and Chen et al. (2012) concluded that the groundwater could not be from local precipitation based on a geochemical study. Previous studies are helpful to understand the groundwater cycle in the plateau. However, these previous studies differ on the origin of the groundwater, probably resulting from the uncertainties of the δD and $\delta^{18}\text{O}$ signals in precipitation due to the effects of the season, altitude and amount (Clark and Fritz, 1997). In addition, current knowledge on geochemical evolution of groundwater is scarce.

The Cretaceous aquifer consists of unconsolidated and porous sandstones and is a dominant groundwater reservoir for drinking and irrigation in the Ordos Desert Plateau (Hou et al., 2008). The infiltration of local precipitation, lateral percolation of river water from the Yellow River and upwelling of deep groundwater are probably the recharge sources to the shallow groundwater in this plateau. Thus, the ions in the shallow groundwater originate from both the recharge sources and the interaction of groundwater with aquifer rocks. The intensity of the water–rock interactions is linked to the source water's composition, the reactivity of the aquifer minerals and the residence time of the groundwater (Gosselin et al., 2004). In this study, we explore the hydrochemical variation in the groundwater, reveal the provenance of the dissolved Sr and evaluate the intensity of the water–rock interactions through the use of Sr isotopes with hydrochemical composition to elucidate the chemical evolution and origin of the shallow groundwater in the Cretaceous aquifer in the Ordos Desert Plateau, North China.

2. Study area

The Ordos Desert Plateau is located between $37^{\circ}35'24''$ and $40^{\circ}51'40''\text{N}$ and between $106^{\circ}42'40''$ and $111^{\circ}27'20''\text{E}$, covering an area of approximately $8 \times 10^4 \text{ km}^2$ with an elevation from 1000 m to 1500 m a.s.l. (above sea level). It is surrounded by the Helan Mts. (>3000 m a.s.l.) to the west, the Yin Mts. (1500–2300 m a.s.l.) to the north, the Luliang Mts. to the east and the Chinese Loess Plateau to the south and is separated from the surrounding mountains by the Yellow River (Fig. 1). The Mu Us sandy land ($37^{\circ}35'–39^{\circ}23'\text{N}$, $107^{\circ}20'–111^{\circ}27'\text{E}$) and the Hobq Desert ($39^{\circ}30'–40^{\circ}41'\text{N}$, $107^{\circ}–111^{\circ}27'\text{E}$) are the major components of the Ordos Desert Plateau (Zhu et al., 1980). The Mu Us sandy land, located in the depression of the southeastern Ordos Desert Plateau, covers an area of $3.2 \times 10^4 \text{ km}^2$ with many semi-stabilized dunes (Fig. 1). The Hobq Desert, which lies on the margin of the northern Ordos Desert Plateau, has an area of $1.61 \times 10^4 \text{ km}^2$ with many mobile dunes.

The Ordos Desert Plateau is arid to semiarid. The annual mean precipitation ranges from 400 mm in the southeast to 150 mm in the northwest, and 60–80% of the precipitation occurs from July to September. The annual mean potential evaporation is high, ranging from 2500 mm to 3000 mm. The annual mean temperature varies between 5.5°C and 9.1°C , with the coldest mean monthly temperature between -13.7°C and -8.9°C and the hottest mean monthly temperature between 21.3°C and 25.4°C (Li, 2001). The climate conditions are distinctly different between the Hobq Desert and Mu Us sandy land (Rao et al., 2009). The Mu Us sandy land has more rainfall and vegetation with weaker winds than the Hobq Desert.

There are several rivers in the Ordos Desert Plateau including the Molin River, Dosit River and Wuding River. The first two are ephemeral while the last is perennial. The rivers are fed by groundwater. In this plateau, there is a >1000 m thick Cretaceous stratum that consists of clastic rocks including sandstone, siltstone and mudstone. The Cretaceous stratum is usually considered to be the main aquifer system. In this aquifer system, there are plenty of groundwater resources. Shallow groundwater is <300 m deep,

while groundwater at a depth of >300 m is generally considered to be deep groundwater (Hou et al., 2008; Su et al., 2011). Shallow groundwater is often utilized by local people for family drinking and agricultural irrigation. According to the watershed conditions (Su et al., 2011; Yin et al., 2011a,b), three groundwater systems are distinguished in this plateau: GWS-1 (Wuding), GWS-2 (Dosit), and GWS-3 (Molin) (Fig. 1). The hydrogeology of the Ordos area has been described in detail by Hou et al. (2008).

3. Sampling and methods

Fifty-six shallow groundwater samples were taken from the Hobq Desert and Mu Us sandy land in the Ordos Desert Plateau and nine river water samples from the nearby Yellow River (Fig. 1). Four weather stations (ETKQQ, ETKQ, WSQ and HJQ) were chosen to collect rainwater samples in the Ordos Desert Plateau (Fig. 1). The HJQ station is located in the Hobq Desert and the other three in the Mu Us sandy land. According to the geographical locations of the stations, the water samples collected at station WSQ, stations ETKQQ and ETKQ, and station HJQ are considered to represent rainwater over GSW-1, GSW-2 and GSW-3, respectively (Fig. 1). The rainwater samplers were cleaned with hydrochloric acid (3 M) and then rinsed with Milli-Q water ($18.2\text{ M}\Omega\text{ cm}$) and dried before sampling. The samplers were placed 2 m above the ground and tightly covered with a plastic lid to avoid any contamination from dry deposition when it did not rain. A total of thirty-eight rainwater samples were collected from the four weather stations during August 2010–July 2011. The pH and total dissolved solid (TDS) values of the water samples were measured by a multi-parametric analyzer (Multi 340i) in the field. The details of the samples are summarized in Table 1 and the supplementary materials ST 1, ST 2 and ST 3.

All the water samples were filtered through a $0.45\text{ }\mu\text{m}$ Millipore membrane filter, and each filtrate was divided into two aliquots. One was stored without further treatment in a 50 mL polyethylene bottle for anion measurement, and the other was acidified with ultra-pure nitric acid to a pH value around 2 and stored in a 250 mL polyethylene bottle for cation measurement and $^{87}\text{Sr}/^{86}\text{Sr}$ ratios. Major anions (Cl^- , SO_4^{2-} and NO_3^-) were measured by ionic chromatography (ICS-2000) and cation measurements (Ca^{2+} , Mg^{2+} , K^+ , Na^+ and Sr^{2+}) were performed by an inductively coupled plasma-atomic emission spectroscopy (ICP-AES, Thermo iCAP 6300) in the State Key Laboratory of Hydrology-Water Resources and Hydraulic Engineering, Hohai University. A blank was prepared for the procedures, including a reagent, filtration and storage, and its test was carried out in parallel with the determination. The analytical precision was better than $\pm 5\%$. The Sr in the water was pre-concentrated by partial evaporation and then purified for Sr isotopic analysis by using standard ion-exchange techniques at the Center of Modern Analysis, Nanjing University. The full procedure blank for this technique is less than 60 pg of Sr. The Sr isotopic determinations were performed on a thermal ionization mass spectrometer (Triton) in the State Key Laboratory of Ore Deposit Geochemistry, Institute of Geochemistry, Chinese Academy of Sciences, China. The reproducibility of the analysis was verified by periodic determinations of the NBS987 strontium standard. The average $^{87}\text{Sr}/^{86}\text{Sr}$ ratio of this standard for 62 determinations was 0.710256 ± 0.000004 (2σ , $n=62$) in the past year.

4. Results

The chemical and Sr isotopic data of the shallow groundwater and other waters including deep groundwater, local rainwater and river water from the nearby Yellow River are listed in Table 1 and the supplementary materials (ST 1, ST 2 and ST 3), respectively.

4.1. Chemical composition

The total dissolved solids (TDS) value of the shallow groundwater is mostly below 1 g/L but varies among the four groundwater systems. The mean TDS value of the shallow groundwater is in the following order: GWS-1 < GWS-2 < GWS-3 and Jizhen, in accordance with the climate conditions (e.g., rainfall and evaporation) over the individual groundwater systems (Yin et al., 2011a). The equivalent ratio of the sum of anions to that of cations ($\Sigma\text{anions}/\Sigma\text{cations}$) can be used to indicate the completeness of the measured major constituents (Al-Khashman, 2005; Li et al., 2007a). HCO_3^- is not measured in this study. The $\Sigma\text{anions}/\Sigma\text{cations}$ ratios vary mostly from 0.1 to 0.6, suggesting that HCO_3^- is missing as a major anion in the shallow groundwater. Ca^{2+} and Mg^{2+} are the dominant cations for most shallow groundwater samples from GWS-1, while Na^+ is dominant for the shallow groundwater samples from GWS-3 and Jizhen (Fig. 2). In addition, the shallow groundwater in GWS-1 appears to have more SO_4^{2-} but less Cl^- compared to that in GWS-3 and Jizhen (Fig. 2). The shallow groundwater in GWS-2 falls geochemically between that in GWS-1 and GWS-3. The Cl^- concentration changes spatially in accordance with the TDS in the shallow groundwater (Table 1).

The TDS value of deep groundwater (>300 m deep) varies from 214 mg/L to 3008 mg/L, with the highest values occurring in GWS-1 and GWS-2 (ST 1). The geochemical differences in the deep groundwater are not significant among GWS-1, GWS-2 and GWS-3. Compared to most of the shallow groundwater samples, the deep groundwater tends to have higher Na^+ and K^+ , but low NO_3^- and variable Cl^- and SO_4^{2-} (Fig. 2). The TDS value of rainwater varies from 12 mg/L to 589 mg/L (ST 2). The volume-weighted mean (VWM) TDS value is 78.84 mg/L, 67.54 mg/L and 108.25 mg/L for the rainwater over GWS-1, GWS-2 and GWS-3, respectively, significantly lower than the shallow groundwater values. Compared to the shallow groundwater, the rainwater tends to have less Mg^{2+} and Cl^- and more SO_4^{2-} (Fig. 2). The TDS value of the Yellow River's water ranging between 342 mg/L and 653 mg/L, and does not greatly change with the seasons (ST 3). However, the samples collected in the summer are characterized by high Ca^{2+} , while those collected in the winter are represented by high Na^+ (ST 3). The Yellow River's water has smaller variations in its geochemical composition, with less Mg^{2+} and NO_3^- than the shallow groundwater (Fig. 2).

4.2. Strontium and its isotopes

Most of the shallow groundwater samples have Sr^{2+} concentrations $<30\text{ }\mu\text{mol/L}$, except for four samples that have values between $37.7\text{ }\mu\text{mol/L}$ and $65.5\text{ }\mu\text{mol/L}$. The Sr^{2+} concentration in the three groundwater systems roughly exhibits a spatial trend, i.e., GWS-1 < GWS-2 < GWS-3 (Table 1). A regular variation in $^{87}\text{Sr}/^{86}\text{Sr}$ ratios can also be observed for the shallow groundwater samples (Fig. 3): the $^{87}\text{Sr}/^{86}\text{Sr}$ ratios are above 0.711 for GWS-1, approximately 0.711 (with one exception of 0.712307) for GWS-2, and between 0.710 and 0.711 (with one exception of 0.711808) for GWS-3 (Table 1). Only one groundwater sample from Jizhen has an $^{87}\text{Sr}/^{86}\text{Sr}$ ratio of 0.71155 (Table 1).

The Sr^{2+} concentrations of the deep groundwater samples are mostly $<30\text{ }\mu\text{mol/L}$ and do not regularly change among the three groundwater systems (ST 1). The $^{87}\text{Sr}/^{86}\text{Sr}$ ratios of the deep groundwater are relatively constant between 0.7106 and 0.7108 in GWS-2 but vary from 0.7098 to 0.7112 in the other groundwater systems (ST 1). Compared to the shallow groundwater, the deep groundwater has a lower Sr isotope value in GWS-1 and GWS-2 but is isotopically similar in GWS-3 (Fig. 3). The Sr^{2+} concentrations in most of the rainwater samples range from $0.06\text{ }\mu\text{mol/L}$ to $6.13\text{ }\mu\text{mol/L}$, except for four high values between $17.05\text{ }\mu\text{mol/L}$ and

Table 1Chemical and Sr isotopic compositons of shallow groundwater in the Ordos Desert Plateau, North China (the unit of ionic concentration is $\mu\text{mol/L}$).

Groundwater system	Sample ID	Sampling date	Longitude	Latitude	Altitude (m)	Well depth (m)	pH	TDS(mg/L)	Cl^-	SO_4^{2-}	NO_3^-	HCO_3^-*	Ca^{2+}	K^+	Mg^{2+}	Na^+	Sr^{2+}	$^{87}\text{Sr}/^{86}\text{Sr}$
GWS-1	WDHZ-1	31-07-2010	108°43'43.0"	37°44'6"	1293	20	7.6	423	1186	868	80.5	4591.0	1760	70.8	1152	1699	8.2	n.d.
	HNL-1	31-07-2010	108°43'0.80"	37°49'49.61"	1234	30	7.8	403	532	2505	39.8	833.8	1270	39.5	1208	1419	8.3	n.d.
	WSZJ-1	04-08-2010	108°57'0.15"	39°25'56.79"	1362	42	8.1	224	511	299	104.5	2341.7	798	29.9	523	885	3.8	n.d.
	LWLTLG-1	25-03-2011	108°58'14.83"	38°39'42.69"	1306	7	7.9	415	1146	1187	1.9	2939.8	2069	30.0	811	673	3.9	n.d.
	TKZ-1	25-03-2011	109°14'26.05"	38°55'15.95"	1297	6	8.5	503	1455	391	2.4	5378.4	1357	135.0	585	3599	3.4	n.d.
	TKZ-2	25-03-2011	109°14'26.05"	38°55'15.95"	1297	50	9.2	396	994	241	3.2	4808.5	1260	175.9	745	2101	3.3	0.711031
	XJZ-1	25-03-2011	109°38'27.32"	39°05'51.58"	1306	6	8.3	355	305	474	395.6	3616.7	1270	33.3	586	1519	5.3	n.d.
	NLXL-1	25-03-2011	109°14'4.96"	39°25'17.36"	1290	3	7.7	415	829	582	153.8	3726.7	517	58.8	656	3470	27.1	n.d.
	SLD-1	26-03-2011	108°53'27.24"	38°28'29.54"	1253	40	8.6	239	443	159	124.5	2828.0	876	16.6	604	737	4.7	0.711140
	XJH-1	26-03-2011	109°33'51.32"	38°26'23.68"	1191	15	8.4	188	146	272	0.9	2284.4	928	25.0	335	425	2.7	n.d.
	WLTLG-1	26-03-2011	109°12'54.89"	38°39'15.94"	1256	20	7.5	203	285	140	62.4	2660.0	468	21.1	747	837	5.8	0.711260
	SRLG-1	27-03-2011	108°37'55.76"	38°06'31.51"	1233	13	9.4	224	178	134	0.5	3265.6	1116	40.1	499	443	3.4	n.d.
	HNX-1	27-03-2011	108°44'5.45"	37°52'15.33"	1234	28	8.8	179	185	227	56.9	2203.8	377	33.8	546	1020	4.4	n.d.
	DXSY-1	2011.07.17	108°09'6.02"	37°46'16.19"	1344	10	8.2	250	390	279	235.1	4374.9	1768	46.7	668	640	5.6	0.711993
	DXSY-2	2011.07.17	108°43'5.06"	37°44'49.05"	1279	40	9.1	239	217	207	160.3	4743.3	1306	77.6	825	1194	5.5	n.d.
	DXSY-3	2011.07.17	108°44'42.72"	37°51'4.09"	1238	70	9	250	488	569	70.5	4133.8	808	36.4	1191	1795	7.4	0.711029
	DXSY-4	2011.07.17	108°42'5.34"	37°52'42.79"	1222	220	8.3	226	364	795	20.7	3276.3	741	49.0	970	1779	8.3	0.711870
	DXSY-5	2011.7.18	108°42'59.64"	37°59'28.51"	1232	40	7.8	364	812	1259	56.0	5693.6	2404	111.9	1427	1307	11.0	0.711132
	DXSY-6	2011.7.18	108°38'56.71"	38°09'26.13"	1252	40	8.1	159	246	261	101.6	3194.0	1426	25.4	375	436	2.8	0.711278
	DXSY-7	2011.7.18	108°42'18.8"	38°13'57.49"	1250	50	8.6	505	2186	757	7.7	8124.0	2185	146.7	1664	3987	10.2	0.711125
	DXSY-8	2011.7.18	108°41'35"	38°24'7.16"	1305	30	7.4	190	178	146	3.2	4767.9	1754	52.6	578	526	3.7	0.711233
	DXSY-9	2011.7.19	108°43'12.53"	38°37'13.03"	1370	60	9.1	262	495	221	208.9	5488.6	2274	76.8	650	709	6.2	0.711734
	DXSY-10	2011.7.19	108°43'27.6"	38°37'7.97"	1342	300	7.8	223	489	206	103.8	5049.6	2053	75.8	631	612	5.1	0.711586
	DXSY-11	2011.7.19	108°34'0.38"	38°43'3.59"	1348	150	8.4	227	313	191	3.2	5544.6	1270	158.9	1113	1319	4.4	n.d.
	DXSY-12	2011.7.19	108°24'33.27"	38°50'49.89"	1368	15	8.1	287	516	407	2.9	6594.8	2553	67.2	798	1158	4.3	n.d.
	ETKQJ-1	28-03-2011	107°32'28.29"	38°10'7.08"	1348	6	8.2	312	287	509	177.4	3239.2	1259	20.7	372	1439	2.3	n.d.
	SMT-1	26-03-2011	108°16'49.73"	38°54'19.42"	1368	8	7.7	332	567	715	52.7	3396.9	1619	33.4	776	624	5.5	n.d.
	ERZQ-1	01-08-2010	107°32'24.72"	38°10'6.38"	1339	40	8	130	200	165	68.4	1542.1	631	35.8	290	263	3.1	n.d.
	ETKQD-1	02-08-2010	107°42'59"	38°53'32.0"	1290	Artesian well	9.3	192	787	461	0.0	793.8	48	6.5	9	2383	0.5	n.d.
	ASZ-1	24-03-2011	107°48'3.72"	39°11'20.18"	1362	10	7.8	910	3715	1319	690.6	3809.7	1830	464.9	2050	2628	13.2	0.711059
	DXSY-13	2011.7.19	108°06'17.66"	39°02'8.55"	1391	22	8.3	229	448	243	128.4	4723.5	998	89.5	908	1887	6.5	n.d.
GWS-2	DXSY-14	2011.7.20	107°57'3.7"	39°01'13.86"	1365	200	8.8	274	943	359	92.9	4964.2	975	80.2	983	2723	8.9	0.711001
	DXSY-15	2011.7.20	107°45'28.84"	38°53'22.83"	1264	Artesian well	7.9	218	945	479	6.3	2357.9	127	22.4	57	3878	1.5	0.712307
	DXSY-16	2011.7.20	107°27'24.87"	38°54'42.8"	1212	40	8	1071	6928	2857	138.2	7872.8	1184	218.3	2472	13122	16.7	n.d.
	DXSY-17	2011.7.20	107°24'36.95"	38°54'5.61"	1211	180	7.6	824	4561	2288	184.5	6992.2	882	133.0	1935	10548	14.0	0.710975
	DXSY-18	2011.7.20	107°13'32.26"	38°29'19.01"	1405	20	8.2	1181	6404	2714	282.0	12600.6	1407	400.3	4066	13370	20.4	0.710839
	DXSY-19	2011.7.20	107°13'41.48"	38°29'20.81"	1407	30	8.6	380	1262	600	37.9	7058.4	1325	496.4	1522	3368	13.8	n.d.
	DXSY-22	2011.7.23	108°52'33.35"	39°52'10.71"	1443	10	8.4	1075	7578	1867	169.7	10914.8	2474	339.0	2428	12252	27.1	0.710084
	DXSY-23	2011.7.23	108°50'42.47"	39°51'42.75"	1425	100	7.7	659	3329	1438	196.9	8744.5	2725	148.9	1825	5896	20.3	0.710319
	DXSY-24	2011.7.23	108°48'34.40"	39°50'46.43"	1403	8	9	553	2747	1168	117.6	8216.8	2247	191.7	1947	4839	37.7	n.d.
	DXSY-25	2011.7.24	108°29'16.38"	40°13'25.50"	1222	5	7.9	355	620	1028	137.8	6744.3	1316	87.9	2263	2313	28.3	n.d.
	DXSY-26	2011.7.24	108°26'48.54"	40°09'7.71"	1176	300	8.1	446	1435	1860	0.8	3002.3	292	46.1	21	7487	38.5	0.710004
	DXSY-27	2011.7.24	108°26'52.00"	40°04'26.73"	1196	150	8.3	409	2038	1045	2.0	3293.0	78	43.3	17	7191	7.8	0.710187
	DXSY-28	2011.7.24	108°33'28.66"	39°58'54.29"	1267	200	7.9	513	2494	1176	55.8	5335.2	456	196.8	766	7596	38.6	n.d.
	DXSY-29	2011.7.26	108°33'17.51"	39°50'54.16"	1331	150	8.1	268	1033	325	118.1	4716.1	855	105.9	1000	2700	65.5	n.d.
GWS-3	DXSY-30	2011.7.26	108°27'51.19"	39°54'13.49"	1218	100	9	212	251	335	1.2	4263.3	282	85.8	959	2617	27.2	0.710322
	DXSY-31	2011.7.26	108°02'9.83"	39°57'36.64"	1228	117	8.5	270	1268	435	85.4	3751.4	681	84.5	684	3160	7.4	0.711808
	DXSY-32	2011.7.26	107°45'15.57"	40°05'12.90"	1169	100	9.3	841	6337	2214	37.4	8322.1	2092	156.7	1066	12652	14.5	0.711046
	DXSY-33	2011.7.26	107°42'53.85"	40°05'11.45"	1190	100	7.8	917	5966	2037	225.9	#####	1865	168.7	1228	14035	14.8	0.710992
	ARSLTJ-1	04-08-2010	108°46'9.96"	39°49'16.37"	1393	8	8	569	3144	1781	332.0	826.9	1018	48.7	1134	3512	12.5	n.d.
	ARSLTJ-1	22-03-2011	108°46'10.26"	39°49'16.11"	1041	10	8.7	642	3113	1767	361.3	2306.0	1167	61.4	1445	4027	16.1	n.d.
	BDJ-1	05-08-2010	108°29'31.30"	40°13'22.00"	1211	4	8.1	322	622	885	213.3	2296.6	652	49.2	1156	1237	16.3	n.d.
	YHWSJ-1	06-08-2010	108°07'34.45"	39°54'17.16"	1285	120	8.3	259	1426	423	116.0	1364.5	453	38.2	643	1522	5.4	n.d.
	BDJ-1	21-03-2011	108°29'31.30"	40°13'22.00"	1211	4	8.4	358	743	1068	184.3	2844.9	724	46.8	1482	1450	20.5	n.d.
JZ	DXSY-20	2011.7.22	107°56'57.35"	40°46'1.99"	1068	10	8.8	325	978	567	147.9	6359.7	####	177.2	####	1687	11.4	0.711550
	DXSY-21	2011.7.22	107°55'9.71"	40°46'3.27"	1031	8	8.5	758	5236	794	71.5	10127.6	####	286.2	####	7413	14.4	n.d.

Note: * HCO_3^- is calculated according to the equivalent balance of cations to anions. n.d. means no determined.

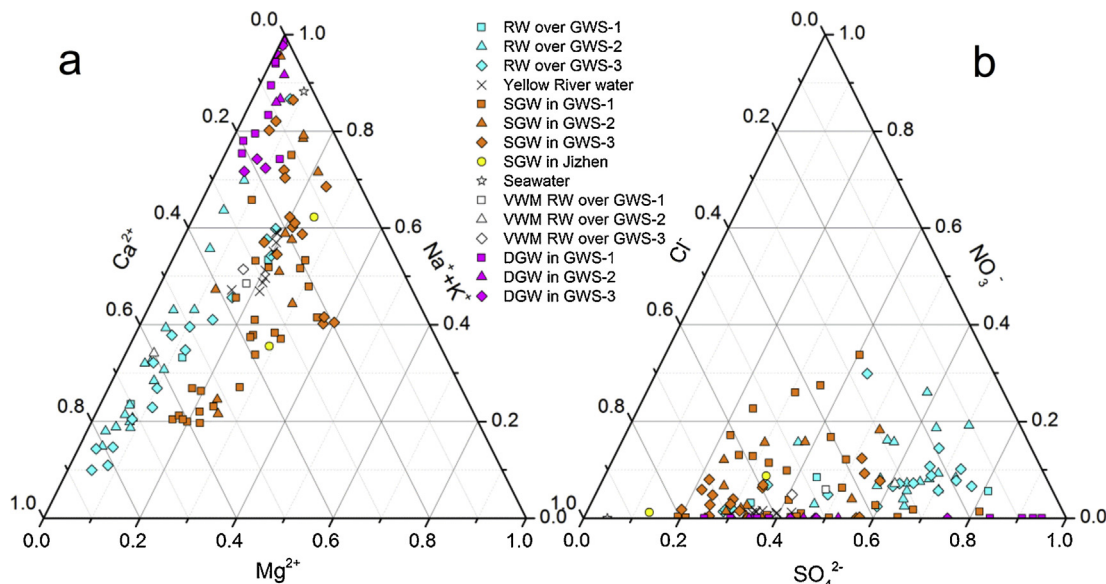


Fig. 2. Ternary diagrams of the hydrochemical compositions of various waters. GWS: groundwater system; RW: rainwater; SGW: shallow groundwater; DGW: deep groundwater; VWM: volume weighted mean. The DGW data are from Su et al. (2011). The seawater data are from Drever (1997).

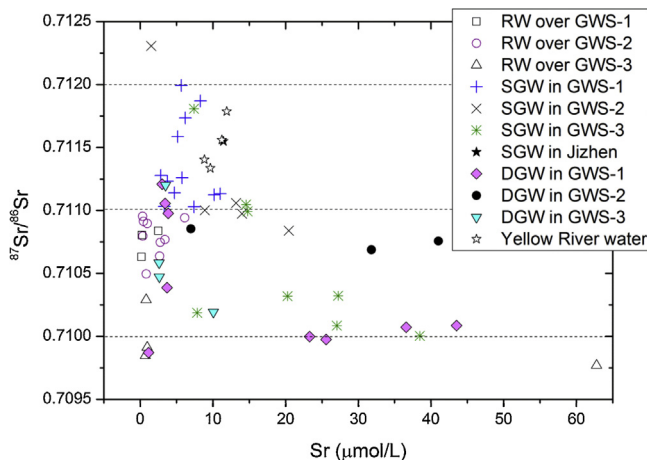


Fig. 3. $^{87}\text{Sr}/^{86}\text{Sr}$ vs. Sr in various waters. The abbreviations in this figure are the same as in Fig. 2 and other figures.

72.19 $\mu\text{mol/L}$ for GWS-3 (ST 2). The high Sr values of these four rainwater samples could be caused by aerosol dust blown up by strong winds in the Hobq Desert area (Wang et al., 2004). The $^{87}\text{Sr}/^{86}\text{Sr}$ ratios fluctuate approximately 0.7107 for the rainwater over GWS-1 and vary from 0.7104 to 0.711 for the rainwater over GWS-2, whereas the rainwater over GWS-3 has $^{87}\text{Sr}/^{86}\text{Sr}$ ratios of 0.7097 to 0.7103, which are slightly lower than those of the first two (Fig. 3). The Sr isotopic variation in the rainwater is identical to that in the shallow groundwater, i.e., higher $^{87}\text{Sr}/^{86}\text{Sr}$ ratios in the Mu Us sandy land and lower $^{87}\text{Sr}/^{86}\text{Sr}$ ratios in the Hobq Desert. The Sr concentration and $^{87}\text{Sr}/^{86}\text{Sr}$ ratio of the Yellow River's water vary from 8.8 $\mu\text{mol/L}$ to 11.9 $\mu\text{mol/L}$ and from 0.7113 to 0.7118, respectively (see ST 3), approaching those of the shallow groundwater in Jizhen and GWS-1 (Fig. 3).

5. Discussion

5.1. Links between the shallow groundwater and other waters

The Ordos Desert Plateau is bounded by the nearby Yellow River from Yinchuan to Baotou to the northwest (Fig. 1). In this plateau, there are a large amount of deep groundwater resources,

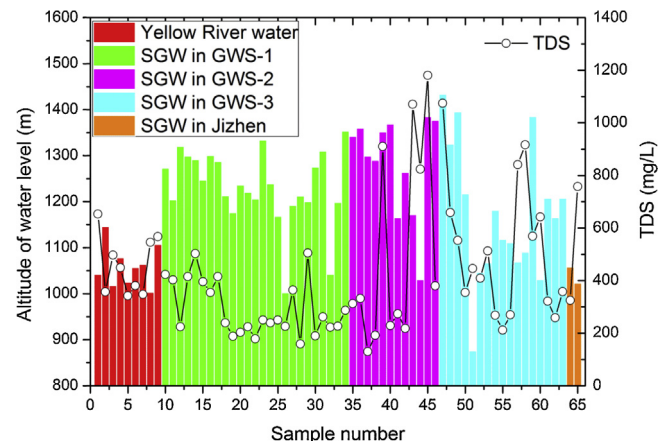


Fig. 4. TDS values and water levels of the water samples from the nearby Yellow River and shallow groundwater samples from the Ordos Desert Plateau.

and the annual mean precipitation ranges spatially from 400 mm to 150 mm (Zhu et al., 1980; Li, 2001). In general, the lateral leakage of river water from the nearby Yellow River, infiltration of local precipitation and upwelling of deep groundwater are considered to be three possible recharge sources for the shallow groundwater in the Ordos Desert Plateau.

The altitude of the nearby Yellow River's water level is between 1100 m and 1003 m, except for higher values at Yinchuan (ST 3 and Fig. 4). The altitudes of the shallow groundwater levels in GWS-1 and GWS-2 are basically greater than 1100 m (Fig. 4). Furthermore, most of the shallow groundwater samples have lower TDS values than the Yellow River's water (Fig. 4). A few shallow groundwater samples from GWS-2 have higher TDS values than the Yellow River water samples; however, the altitudes of the water levels of these groundwater samples are apparently higher than those of the Yellow River's water samples. Therefore, although the river water and some shallow groundwater samples have similar Sr isotopic and geochemical compositions (Figs. 2–3), the nearby Yellow River is not a recharge source of the shallow groundwater in the Ordos Desert Plateau. It is worth noting that the shallow groundwater in Jizhen along the right bank of the Yellow River has similar Sr

isotopic and chemical compositions to the Yellow River's water, and the altitude of the groundwater level is identical to that of the Yellow River's water level (Figs. 2–4). Thus, it is possible that the shallow groundwater in Jizhen is recharged by the lateral leakage of river water from the Yellow River.

The geochemical differences between the shallow and deep groundwater are observed in Fig. 2. Moreover, the $^{87}\text{Sr}/^{86}\text{Sr}$ ratios are lower in the deep groundwater than in the shallow groundwater for GWS-1 and GWS-2 and roughly similar between the deep and shallow groundwater for GWS-3 (Fig. 3). In addition, the deep groundwater, which has a ^{14}C age of at least several thousand years and is depleted in ^2H and ^{18}O compared to the local precipitation (Hou et al., 2007; Yin et al., 2010, 2011a,b), has been evidenced to be of meteoric origin in the geologic past (Hou et al., 2007; Yin et al., 2010). In contrast, the shallow groundwater, which has an age of less than 100 years and is enriched in ^2H and ^{18}O compared to the deep groundwater, is suggested to be recharged by modern precipitation (Hou et al., 2007; Liu et al., 2007; Yin et al., 2010). Therefore, the shallow groundwater is not related to the deep groundwater in the Ordos Desert Plateau.

As a result, the shallow groundwater is only recharged by local precipitation in the Ordos Desert Plateau because the nearby Yellow River and deep groundwater are ruled out. Most previous studies stressed the importance of local precipitation to groundwater, while a few authors speculated that there exists an unknown source of groundwater (Hou et al., 2008; Yin et al., 2010, 2011a,b; Chen et al., 2012), supporting our conclusion.

5.2. Causes of hydrochemical variation between rainwater and shallow groundwater

Because the shallow groundwater is recharged by local precipitation through unsaturated zones or rock fractures and reacts with aquifer rocks, its chemical composition is controlled by water–rock interactions in addition to local precipitation. Cretaceous sandstone is the main aquifer rock in the Ordos Desert Plateau, comprising evaporites, carbonates and silicates (Hou et al., 2007; Liu et al., 2007). Evaporite and carbonate dissolution and silicate hydrolysis are the most likely mechanisms controlling the hydrochemical variation in the shallow groundwater.

The Cl^-/Na^+ and $\text{SO}_4^{2-}/\text{Na}^+$ ratios of the shallow groundwater are mostly <1 and are lower than those of rainwater (Fig. 5a), showing additional Na^+ in the shallow groundwater. Na^+ in the shallow groundwater usually comes from evaporite (halite, sea salt and mirabilite) dissolution, silicate weathering and anthropogenic pollution in addition to the recharge source. If the shallow groundwater is anthropogenically polluted, Cl^-/Na^+ , $\text{SO}_4^{2-}/\text{Na}^+$ and $\text{NO}_3^-/\text{Na}^+$ should be >1 . Therefore, Cl^-/Na^+ and $\text{SO}_4^{2-}/\text{Na}^+$, which are of <1 , show that most of the shallow groundwater samples are not polluted by human beings (Fig. 5a). As a typical proxy for evaluating water pollution, the $\text{NO}_3^-/\text{Na}^+$ value is also <1 (Fig. 5b), supporting this conclusion. The $\text{SO}_4^{2-}/\text{Cl}^-$ value decreases as the SO_4^{2-} concentration increases from the rainwater to the shallow groundwater, implying halite or sea salt dissolution (Fig. 5d). If the Na^+ comes from halite, sea salt or mirabilite, Cl^- and SO_4^{2-} should balance its charge in the groundwater. However, the observed Cl^-/Na^+ and $\text{SO}_4^{2-}/\text{Na}^+$ for most of the shallow groundwater samples are significantly <1 , which is probably a combination of halite, sea salt and mirabilite dissolution. Alternatively, the weathering of Na-silicates (e.g., albite) can result in increasing of Na^+ in shallow groundwater. Nevertheless, previous studies noted that the chemical weathering in the arid and semi-arid areas in North China is mainly carbonate dissolution (Rao et al., 2009). Thus, silicate weathering could be weak in the aquifers. Gypsum dissolution could not occur because (1) $\text{SO}_4^{2-}/\text{Na}^+$, $\text{Mg}^{2+}/\text{Ca}^{2+}$, and $\text{SO}_4^{2-}/\text{Cl}^-$ decrease from rainwater to shallow groundwater

(Fig. 5a–d); (2) the samples plot well over the gypsum dissolution line (Fig. 5e); (3) gypsum is not widespread in aquifers; and (4) the saturation indices computed by the PHREEQC geochemical code (Parkhurst and Appelo, 1999) vary from -1.7 to -3.58 , indicating that the shallow groundwater is undersaturated with respect to gypsum. As a result, the low Cl^-/Na^+ and $\text{SO}_4^{2-}/\text{Na}^+$ of most shallow groundwater samples are caused by the progressive interaction of water with various minerals (halite, mirabilite and albite) in aquifers (Venturelli et al., 2003). Samples LWLTLG-1 and ASZ-1, which have Cl^-/Na^+ values >1 , could be affected by anthropogenic pollution (Fig. 5a).

Sr^{2+} is geochemically similar to Ca^{2+} and usually resides in carbonates and K- or Ca-silicates (Capo et al., 1998). The Sr^{2+} and Ca^{2+} concentrations are basically higher in the shallow groundwater than in the rainwater, suggesting the existence of carbonate dissolution and/or silicate hydrolysis (Fig. 5e). Most of the groundwater samples from GWS-3 and a few groundwater samples from GWS-1 and GWS-2 fall above the seawater dilution line, whereas all other samples are between the seawater line and the calcite line (Fig. 5e). For the groundwater above the seawater line, the hydrolysis of silicate minerals with high $\text{Sr}^{2+}/\text{Ca}^{2+}$ could be an important factor. Second, the rainwater above the seawater line could be a sole source for the groundwater chemistry above the seawater line through direct recharge. Third, for the groundwater between the seawater line and calcite line, the mixing of the dissolved products of various minerals, particularly calcite and dolomite, could have a dominant influence after rainfall. The shallow groundwater has a similar $\text{Sr}^{2+}/\text{Ca}^{2+}$ range to the rainwater, but they apparently have different $\text{Sr}^{2+}/\text{Mg}^{2+}$ (Fig. 5f). The lower $\text{Sr}^{2+}/\text{Mg}^{2+}$ value in the shallow groundwater than in the rainwater reflects dolomite dissolution in aquifers. This conclusion is consistent with that obtained from the major ion ratios. The saturation indices of the groundwater samples with respect to calcite and dolomite, which are computed by the PHREEQC geochemical code (Parkhurst and Appelo, 1999), vary from -0.56 to 1.78 and from -1.78 to 3.57 , respectively, and are mostly >0 . Thus, most groundwater samples are oversaturated with respect to carbonates, further demonstrating the importance of carbonate dissolution in groundwater. On the other hand, a few groundwater samples, particularly from GWS-2 and GWS-3, seem to lie close to the data cluster of rainwater, probably suggesting weak water–rock interactions (Fig. 5f).

5.3. Sr isotopic constraints on the provenance of the Sr in the shallow groundwater

In general, two types of groundwater can be differentiated by the $^{87}\text{Sr}/^{86}\text{Sr}$ ratio. One type has an $^{87}\text{Sr}/^{86}\text{Sr}$ ratio higher than 0.725 and the other has an $^{87}\text{Sr}/^{86}\text{Sr}$ ratio significantly lower than 0.725 (Franklyn et al., 1991; Land et al., 2000; Harrington and Herczeg, 2003; Bishop et al., 1994; Armstrong et al., 1998; Deng et al., 2009). The former are waters that have interacted with aquifer rocks with high $^{87}\text{Sr}/^{86}\text{Sr}$ ratios, whereas the latter are waters that have interacted with aquifer rocks with low $^{87}\text{Sr}/^{86}\text{Sr}$ ratios. The shallow groundwater in the Ordos Desert Plateau belongs to the latter.

The residual fractions (after the removal of extractable Sr by 0.5 M HOAc solution) of the Cretaceous sandstones—the main aquifer rocks, have $^{87}\text{Sr}/^{86}\text{Sr}$ ratios between 0.713 and 0.723 in the Ordos Desert Plateau (Rao et al., 2011). Because the 0.5 M HOAc solution only dissolves carbonates (Yang et al., 2000), the residual fractions of the sandstones may be regarded as the silicate fractions of the aquifer rocks. No Sr isotope data have been reported for the soluble fractions of sandstones until now. Rao et al. (2009) reported that surface carbonates have $^{87}\text{Sr}/^{86}\text{Sr}$ ratios between 0.7101 and 0.7108 in the Hobq Desert and between 0.7110 and 0.7114 in the Mu Us sandy land. Surface carbonates were extracted from the surface sand by using the same leaching method as that of Rao et al.

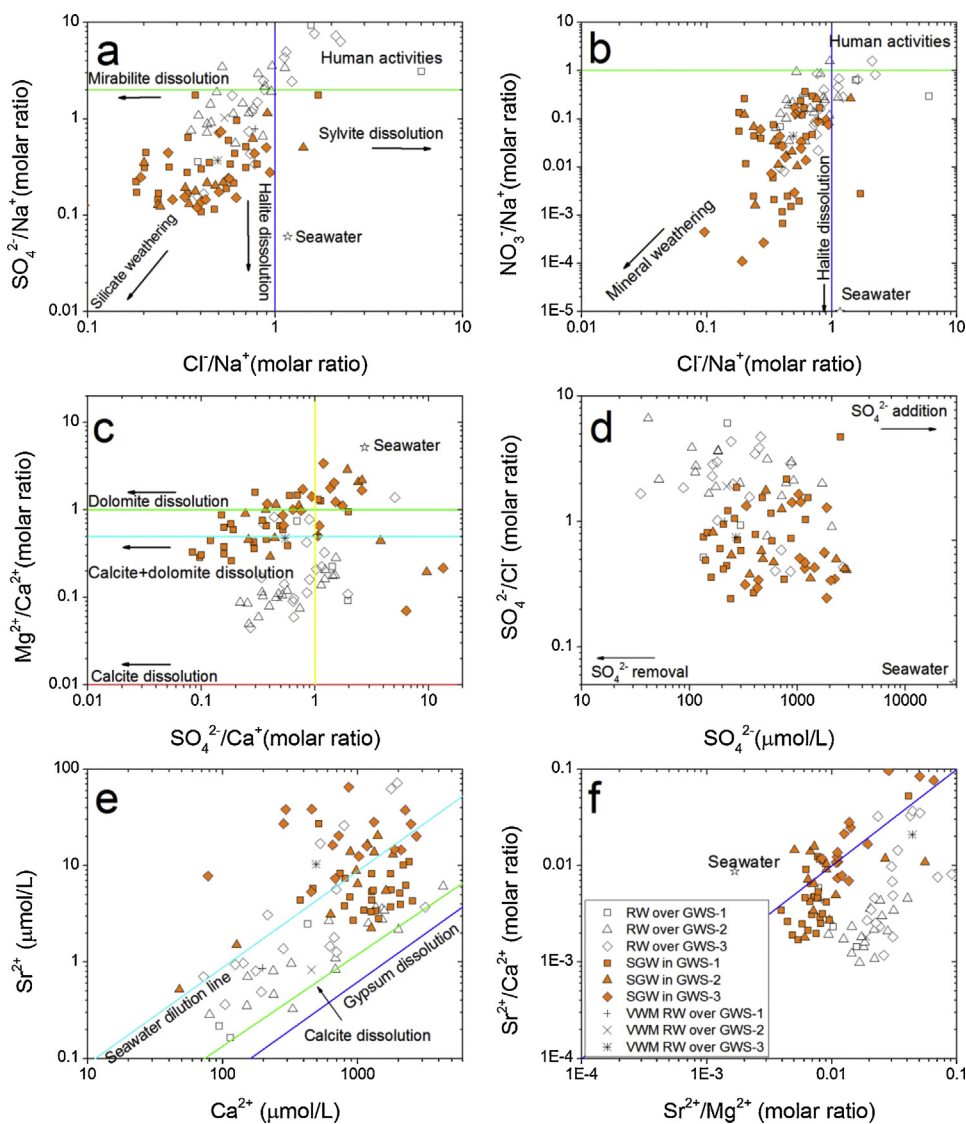


Fig. 5. Pair diagrams of the ion ratios. The seawater data are from Drever (1997). The legends of (a–e) are the same as that of (f).

(2011). Furthermore, the surface sand originated from the weathering of sandstones in the Ordos Desert Plateau (Zhu et al., 1980). Therefore, the surface carbonates may be considered as the carbonate fractions of the aquifer rocks. Carbonate dissolution and silicate weathering of aquifer rocks, together with local precipitation, are probably the Sr sources of the shallow groundwater in the Ordos Desert Plateau.

The Sr sources that might control the $^{87}\text{Sr}/^{86}\text{Sr}$ ratio can be constrained by the relationships between the Sr isotopic composition and concentration ratios (Négrel, 1999; Roy et al., 1999; Hogan et al., 2000). Fig. 6 shows the relationship in an $^{87}\text{Sr}/^{86}\text{Sr}$ vs. $1/\text{Sr}$ diagram. Three end-members of the shallow groundwater can be observed from Fig. 6: (a) silicate fractions of aquifer rocks (RS), characterized by high $^{87}\text{Sr}/^{86}\text{Sr}$ and low $1/\text{Sr}$ ratios; (b) carbonate fractions of aquifer rocks (SC), represented by low $^{87}\text{Sr}/^{86}\text{Sr}$ and $1/\text{Sr}$ ratios; and (c) local rainwater, characterized by low $^{87}\text{Sr}/^{86}\text{Sr}$ and high $1/\text{Sr}$ ratios. For GWS-1, the binary mixing line connecting the carbonate fractions of the aquifer rocks (Mean SC in Mu Us) to the local rainwater (VWM RW over GWS-1) reflects the control of carbonate dissolution and local rainwater on the Sr in the shallow groundwater (Fig. 6b). Fig. 6b clearly shows that some samples plot directly on and near the mixing line. This mixing line includes TKZ-2, SLD-1, DXSY-3, DXSY-5 and DXSY-7

(Table 1). All the other samples points lie within the triangle whose apexes are local rainwater (VWM RW over GWS-1) and the carbonate and silicate fractions (Mean SC and RS in Mu Us). Overall, all the sample points plot apparently closer to the carbonate fraction end-member than to the other two end-members, indicating the importance of carbonate dissolution to the Sr in the shallow groundwater (Fig. 6b). For GWS-2, most of the shallow groundwater samples also plot near the carbonate fraction end-member (Mean SC in Mu Us), reflecting the control of carbonate dissolution on the Sr in the shallow groundwater (Fig. 6b). Exceptionally, sample DXSY-15 falls among all three end-members, namely, local rainwater (VWM RW over GWS-2), the carbonate and silicate fractions of aquifer rocks (Mean SC and RS in Mu Us), suggesting the mixing contribution of the three end-members to Sr in this sample (Fig. 6b). For GWS-3, four samples, DXSY-22, DXSY-23, DXSY-26 and DXSY-30, plot near the mixing line connecting local rainwater (VWM RW over GWS-3) and the carbonate fractions of aquifer rocks (Mean SC in Hobq), indicating the predominance of local rainwater and carbonate dissolution (Fig. 6b). Samples DXSY-32 and DXSY-33 fall within the triangle whose apexes are local rainwater (VWM RW over GWS-3) and the carbonate and silicate fractions of aquifer rocks (Mean SC and RS in Hobq), showing the common effects of the end-members (Fig. 6b). Samples DXSY-27 and DXSY-31 lie outside

Table 2

mean $^{87}\text{Sr}/^{86}\text{Sr}$ ratios and Sr concentrations ($\mu\text{g/g}$ for aquifer rock and mg/L for water) of various end-members for three groundwater systems.

Source	End-members	GWS-1		GWS-2		GWS-3	
		$^{87}\text{Sr}/^{86}\text{Sr}$	Sr	$^{87}\text{Sr}/^{86}\text{Sr}$	Sr	$^{87}\text{Sr}/^{86}\text{Sr}$	Sr
Local precipitation	Rainwater (RW)	0.710760	0.0765	0.710844	0.0726	0.709967	0.911
Aquifer rock	Residual sandstones (RS)	0.716552	284	0.716552	284	0.717433	266
	Carbonate-mainly composed of calcite (SC)	0.711176	3.37	0.711176	3.37	0.710425	27.6

Note: the volume weighted values are calculated for the rainwater end-member according to Sr isotopic data, Sr concentrations and the amount of rainwater which are presented in ST 2. The arithmetical values are used for the other two end-members (i.e., RS and SC) and SC is represented by the values of surface calcite, original Sr data are from Rao et al. (2009, 2011).

Table 3

Relative contributions of Sr from various end-members to shallow groundwater.

Groundwater system	Sample ID	Groundwater $^{87}\text{Sr}/^{86}\text{Sr}$	Groundwater Sr (mg/L)	Calculated values			Calibrated values		
				X_{RW}	X_{SC}	X_{RS}	X_{RW}	X_{SC}	X_{RS}
GWS 1	TKZ-2*	0.711031	0.29	26.3%	74.4%	-0.7%	73.7%	0%	
	SLD-1	0.71114	0.41	18%	81%	1%			
	WLTLG-1	0.71126	0.51	15.1%	82.2%	3%			
	DXSY-1	0.711993	0.50	15.4%	68.2%	16.4%			
	DXSY-3*	0.711029	0.65	12%	90%	-2%	88%	0%	
	DXSY-4	0.71187	0.73	10.5%	75.8%	13.7%			
	DXSY-5*	0.711132	0.97	7.9%	92.3%	-0.2%	92.1%	0%	
	DXSY-6	0.711278	0.25	30.8%	64.9%	4.3%			
	DXSY-7*	0.711125	0.90	8.5%	91.8%	-0.3%	91.5%	0%	
	DXSY-8	0.711233	0.33	23.2%	73.9%	2.9%			
	DXSY-9	0.711734	0.55	14.0%	74.5%	11.5%			
	DXSY-10	0.711586	0.45	16.9%	74.2%	8.9%			
	ASZ-1*	0.711059	1.16	6.3%	95.5%	-1.8%	93.7%	0%	
	DXSY-14*	0.711001	0.78	9.3%	93.4%	-2.7%	90.7%	0%	
GWS 2	DXSY-15	0.712307	0.13	54.7%	20.9%	24.4%			
	DXSY-17*	0.710975	1.23	5.9%	97.5%	-3.4%	94.1%	0%	
	DXSY-18*	0.710839	1.80	4%	102%	-6%	96%	0%	
	DXSY-22*	0.710084	2.38	38.3%	64.1%	-2.4%	61.7%	0%	
	DXSY-23	0.710319	1.78	51.1%	47.1%	1.8%			
	DXSY-26*	0.710004	3.38	26.9%	77.3%	-4.2%	73.1%	0%	
GWS 3	DXSY-27#	0.710187	0.69	132.5%	-37.8%	5.3%	100%	0%	0%
	DXSY-30	0.710322	2.40	38.0%	61%	1.0%			
	DXSY-31#	0.711808	0.65	140.2%	-69.1%	28.9%	?	?	?
	DXSY-32	0.711046	1.28	71.2%	15.3%	13.5%			
	DXSY-33	0.710992	1.30	70.1%	17.2%	12.7%			

Note: the calibrated values are available for samples marked by * and #, and the calculated values for samples without symbols.

this triangle (Fig. 6b). DXSY-31 is probably impacted by additional sources. DXSY-27 could not have experienced water–rock interactions because it approaches the local rainwater end-member (VWM RW over GWS-3).

5.4. Quantifying water–rock interactions by Sr isotopes

$^{87}\text{Sr}/^{86}\text{Sr}$ ratios are commonly used alongside Sr concentrations to construct a simple model to quantify the geochemical contributions of various end-members to groundwater and evaluate the water–rock interactions (Frost and Toner, 2004; Négrel et al., 2001). Because the local precipitation and carbonate and silicate fractions of aquifer rocks are the three end-members controlling the chemical composition of the shallow groundwater in the Ordos Desert Plateau, their relative contributions of Sr to the shallow groundwater can be calculated by using the following equations:

$$X_{\text{RW}} + X_{\text{SC}} + X_{\text{RS}} = 1 \quad (1)$$

$$[\text{Sr}^{2+}]_{\text{RW}} \times X_{\text{RW}} + [\text{Sr}^{2+}]_{\text{SC}} \times X_{\text{SC}} + [\text{Sr}^{2+}]_{\text{RS}} \times X_{\text{RS}} = [\text{Sr}^{2+}]_{\text{GW}} \quad (2)$$

$$(^{87}\text{Sr}/^{86}\text{Sr})_{\text{RW}} \times X_{\text{RW}} + (^{87}\text{Sr}/^{86}\text{Sr})_{\text{SC}} \times X_{\text{SC}} + (^{87}\text{Sr}/^{86}\text{Sr})_{\text{RS}} \times X_{\text{RS}} = (^{87}\text{Sr}/^{86}\text{Sr})_{\text{GW}} \quad (3)$$

where GW, RW, SC and RS refer to the shallow groundwater, local rainwater, carbonate fraction (represented by surface calcite) and silicate fraction (represented by residual sandstone), respec-

tively; $[\text{Sr}^{2+}]$ is the strontium concentration; and X stands for the relative Sr contribution from the end-member.

The parameters of the three end-members controlling the shallow groundwater's chemistry are listed in Table 2. The relative Sr contributions of the end-members to the shallow groundwater are calculated and presented in Table 3.

As listed in Table 3, the calculated X_{RS} values for the samples marked with * are slightly negative, indicating that the silicate weathering of aquifer rocks is insignificant to the chemical compositions of these samples. These samples plot along the mixing lines connecting local rainwater (RW) to the carbonate fraction (SC) of the aquifer rocks, as shown in Fig. 6b. Therefore, the relative Sr contributions of the end-members for these samples should be calculated by a binary mixing model (Négrel et al., 2004), and the calibrated values of X_{SC} are listed in Table 3.

DXSY-27 and DXSY-31 have lower Sr concentrations than the volume weighted value of rainwater (Tables 2 and 3). Sample DXSY-27 plots near the volume weighted value of rainwater and thus may be considered to completely inherit the geochemical nature of the local precipitation (Fig. 6b). Sample DXSY-31 plots far from the end-member RW and outside of the RW-SC-SR field and is probably affected by unknown sources (Fig. 6b).

For GWS-1, the relative Sr contribution from local rainwater (X_{RW}) varies from 7.9% to 30.8%, that from carbonate dissolution

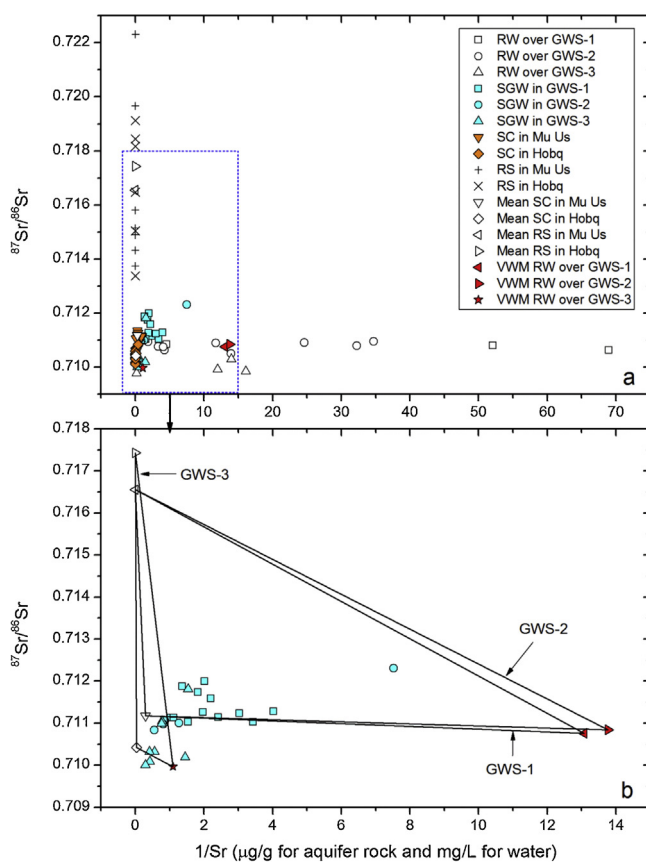


Fig. 6. $^{87}\text{Sr}/^{86}\text{Sr}$ vs. $1/\text{Sr}$ of the shallow groundwater in the Ordos Desert Plateau and various end-members. SC—carbonate fraction; RS—silicate fraction.

(X_{SC}) varies from 68.2% to 92.3% and that from silicate weathering (X_{RS}) varies from 0% to 16.4% (Table 3). The Sr in the shallow groundwater chiefly comes from carbonate dissolution, followed by local precipitation. For GWS-2, sample DXSY-15 receives up to 24.4% of its Sr from residual sandstone weathering and up to 54.6% from the local precipitation, respectively; however, most of the samples are geochemically dominated by carbonate dissolution because X_{SC} is >90% (Table 3). The relative Sr contributions from the individual end-members in GWS-3 are greatly distinct from those in GWS-1 and WS-2 (Table 3). Samples DXSY-22, DXSY-26 and DXSY-30 have <40% Sr from local precipitation, whereas the other groundwater samples except for DXSY-31 receive Sr mainly from local precipitation. It is worth noting that more than 10% of the Sr for two shallow groundwater samples (DXSY-32 and DXSY-33) originates from silicate weathering. As a whole, these results indicate that (1) the water–rock interactions are mainly characterized by strong carbonate dissolution and weak silicate weathering for most of the shallow groundwater samples; (2) the intensity of the water–rock interactions varies among the three groundwater systems (GWS-1, -2 and -3), and even within each groundwater system.

The spatial variations in the intensity of the water–rock interactions could be associated with the residence times or flow rates of the shallow groundwater and chemical nature of the rainwater because the lithology of the aquifer rocks is spatially similar in the Ordos Desert Plateau (Hou et al., 2008). A previous study using CFCs as dating tools showed that the shallow groundwater has an age of ca. 20 a in the Ordos Desert Plateau (Liu et al., 2007). Assuming this groundwater age of 20 a, the flux of Sr released from the aquifer rocks to the shallow groundwater should vary roughly from 0.011 to 0.045 $\mu\text{g}/\text{mL}/\text{y}$ for GWS-1, from 0.003 to 0.086 $\mu\text{g}/\text{mL}/\text{y}$ for GWS-

2 and from 0 to 0.124 $\mu\text{g}/\text{mL}/\text{y}$ for GWS-3. This result reflects the great variability of aquifer weathering to a certain extent.

6. Conclusions

Shallow groundwater is an important water resource in the Ordos Desert Plateau where there are a semi-arid climate and a large population. In this study, the chemical and Sr isotopic compositions of the shallow groundwater in this region are investigated in detail and several conclusions are obtained as follows:

- (1) The total dissolved solids (TDS) value in the shallow groundwater, generally below 1 g/L, is lowest in GWS-1 and highest in GWS-3. Ca^{2+} and Mg^{2+} are the dominant cations in the shallow groundwater for GWS-1, while Na^+ is dominant for GWS-3. The Sr^{2+} concentration has the same variation as TDS in the shallow groundwater. The $^{87}\text{Sr}/^{86}\text{Sr}$ ratio of the shallow groundwater varies spatially in the following order: GWS-3 (between 0.710 and 0.711) < GWS-2 (~0.711) < GWS-1 (>0.711).
- (2) The river water from the nearby Yellow River, which is characterized by high Ca^{2+} in the summer and high Na^+ in the winter, has an $^{87}\text{Sr}/^{86}\text{Sr}$ ratio of 0.7113–0.7117. The $^{87}\text{Sr}/^{86}\text{Sr}$ ratio of the deep groundwater is lower than that of the shallow groundwater for GWS-1 and GWS-2 and roughly similar to that of the shallow groundwater for GWS-3. According to the water levels, hydrochemical and Sr isotopic data in combination with the D-O isotopes and groundwater ages, local precipitation is the main recharge source of the shallow groundwater in the Ordos Desert Plateau.
- (3) The shallow groundwater's chemistry is controlled by two factors: local precipitation and water–rock interactions. The ionic ratios show that three end-members are responsible for the shallow groundwater's chemistry: local precipitation, evaporite and carbonate dissolution, and silicate hydrolysis. The Sr isotope ratios further indicate that the processes occurring in the aquifer are mainly carbonate dissolution rather than silicate hydrolysis.
- (4) The results of Sr isotope mass balance show that >70% of the Sr for most shallow groundwater samples in GWS-1 and GWS-2 is contributed by carbonate dissolution. Three groundwater samples (DXSY-22, -26 and -30) have <40% relative Sr contributions from local precipitation, whereas other groundwater samples except for DXSY-31 have >50% relative Sr contributions from local precipitation in GWS-3. The spatial variation in the intensity of the water–rock interactions could be related to the residence time or flow rate of shallow groundwater, in addition to the chemical properties of the local rainwater.

Acknowledgments

The authors would like to thank Jiang Sun, Xiao Wang and Yaodong Pan for their field help. Thanks are also given to Xiaobiao Li and Xue Sun for Sr isotopic and hydrochemical analyses. This study is financially supported by the National Natural Science Foundation of China (Grant Nos. 40973001, 41273015, 41271041).

Appendix A. Supplementary data

Supplementary data associated with this article can be found, in the online version, at <http://dx.doi.org/10.1016/j.chemer.2015.07.003>

References

- Al-Khashman, O.A., 2005. Ionic composition of wet precipitation in the Petra Region, Jordan. *Atmos. Res.* 78, 1–12.
- Armstrong, S.C., Sturchio, N.C., Hendry, M.J., 1998. Strontium isotopic evidence on the chemical evolution of pore waters in the Milk River Aquifer, Alberta, Canada. *Appl. Geochem.* 13, 463–475.
- Bishop, P.K., Smalley, P.C., Emery, D., Dickson, J.A.D., 1994. Strontium isotopes as indicators of the dissolving phase in a carbonate aquifer: implications for ^{14}C dating of groundwater. *J. Hydrol.* 154, 301–321.
- Capo, R.C., Stewart, B.W., Chadwick, O.A., 1998. Strontium isotopes as tracers of ecosystem processes: theory and methods. *Geoderma* 82, 197–225.
- Cartwright, I., Weaver, T., Petrides, B., 2007. Controls on $^{87}\text{Sr}/^{86}\text{Sr}$ ratios of groundwater in silicate-dominated aquifers: SE Murray Basin, Australia. *Chem. Geol.* 246, 107–123.
- Chen, J.S., Liu, X.Y., Wang, C.Y., Rao, W.B., Tan, H.B., Dong, H.Z., Sun, X.X., Wang, Y.S., Su, Z.G., 2012. Isotopic constraints on the origin of groundwater in the Ordos Basin of northern China. *Environ. Earth Sci.* 66, 505–517.
- Clark, I., Fritz, P., 1997. *Environmental Isotopes in Hydrogeology*. Lewis Publishers, U.S. pp. 1–352.
- de Caritat, P., Kirste, D., Carr, G., McCulloch, M., 2005. Groundwater in the Broken Hill region, Australia: recognizing interaction with bedrock and mineralization using S , Sr and Pb isotopes. *Appl. Geochem.* 20, 767–787.
- Deng, Y.M., Wang, Y.X., Ma, T., 2009. Isotope and minor element geochemistry of high arsenic groundwater from Hangjinhouqi, the Hetao Plain, Inner Mongolia. *Appl. Geochem.* 24, 587–599.
- Drever, J.I., 1997. *The Geochemistry of Natural Waters: Surface and Groundwater Environments*. Prentice-Hall, Englewood Cliffs, NJ.
- Faure, G., 1991. *Principles and Applications of Inorganic Geochemistry*. Prentice-Hall, New Jersey, pp. 626.
- Feng, Q., Cheng, G.D., Masao, M.K., 2000. Trends of water resource development and utilization in arid north-west China. *Environ. Geol.* 39 (8), 831–838.
- Franklyn, M.T., McNutt, R.H., Kamineni, D.C., Gascoyne, M., Frape, S.K., 1991. Groundwater $^{87}\text{Sr}/^{86}\text{Sr}$ values in the Eye-Dashwa Lakes pluton, Canada: evidence for plagioclase-water reaction. *Chem. Geol.* 86, 111–122.
- Frost, C.D., Toner, R.N., 2004. Strontium isotopic identification of water–rock interaction and groundwater mixing. *Groundwater* 42, 418–432.
- Gosselin, Harvey, D.C., Frost, F.E., Stotler, C., R, Macfarlane, P.A., 2004. Strontium isotope geochemistry of groundwater in the central part of the Dakota (Great Plains) aquifer. *USA. Appl. Geochem.* 19, 359–377.
- Harrington, G.A., Herczeg, A.L., 2003. The importance of silicate weathering of a sedimentary aquifer in arid Central Australia indicated by very high $^{87}\text{Sr}/^{86}\text{Sr}$ ratios. *Chem. Geol.* 199, 281–292.
- Hogan, J.F., Blum, J.D., Siegel, D.I., Glaser, P.H., 2000. $^{87}\text{Sr}/^{86}\text{Sr}$ as a tracer of groundwater discharge and precipitation recharge in the Glacial Lake Agassiz, Peatlands, northern Minnesota. *Water Resour. Res.* 36, 3701–3710.
- Hou, G.C., Wang, D.Q., Yin, L.H., 2004. Groundwater systems in the Ordos Basin. In: *Guangcai, H., Maosheng, Z. (Eds.), Groundwater Resources and Its Utilization in the Ordos Basin*. Xi'an: Shaanxi Science and Technology Press, pp. 28–38 (in Chinese with English Abstract).
- Hou, G.C., Su, X.S., Lin, X.Y., Liu, F.T., Yi, S.P., Dong, W.H., Yu, F.K., Yang, Y.C., Wang, D., 2007. Environmental isotopic composition of natural water in Ordos Cretaceous Groundwater Basin and its significance for hydrological cycle. *Acta Geol. Sin.* 37 (2), 255–260 (in Chinese with English Abstract).
- Hou, G.C., Liang, Y.P., Su, X.S., Zhao, Z.H., Tao, Z.P., Yin, L., Yang, H., Wang, Y.C., 2008. Groundwater systems and resources in the Ordos Basin, China. *Acta Geol. Sin.* 82 (5), 1061–1069.
- Kossert, K., 2003. Half-life measurements of ^{87}Rb by liquid scintillation counting. *Appl. Radiat. Isot.* 59 (5–6), 377–382.
- Land, M., Ingri, J., Andersson, P.S., Öhlander, B., 2000. Ba/Sr , Ca/Sr and $^{87}\text{Sr}/^{86}\text{Sr}$ ratios in soil water and groundwater: implications for relative contributions to stream water discharge. *Appl. Geochem.* 15, 311–325.
- Li, X.R., 2001. Study on shrub community diversity of Ordos Plateau, Inner Mongolia, northern China. *J. Arid Environ.* 47, 271–279.
- Li, C., Kang, S., Zhang, Q., Kaspari, S., 2007a. Major ionic composition in the Nam co region, Central Tibetan Plateau. *Atmos. Res.* 85, 351–360.
- Li, W.P., Zhou, H.C., Zhou, Y.X., 2007b. *Typical Groundwater Flow System in Arid northwestern China*, 179. Beijing Seismological Press (in Chinese with English Abstract).
- Liu, F.T., Su, X.S., Hou, G.C., Lin, X.Y., Yi, S.P., Dong, W.H., 2007. Application of CFCs methods in dating shallow groundwater in the Ordos Cretaceous Groundwater Basin. *J. Jilin Univ. (Earth Sci. Ed.)* 37 (2), 298–302 (in Chinese with English Abstract).
- McNutt, R.H., 2000. Strontium isotopes. In: Cook, P.G., Herczeg, A.L. (Eds.), *Environmental Tracers in Subsurface Hydrology*. Kluwer Academic Publishers, Boston, pp. 233–260.
- Négrel, P., 1999. Geochemical study of a granitic area—the Margeride Mountains, France: chemical element behavior and $^{87}\text{Sr}/^{86}\text{Sr}$ constraints. *Aquat. Geochem.* 5, 125–165.
- Négrel, P., Casanova, J., Aranyossy, J.F., 2001. Strontium isotope systematics used to decipher the origin of groundwaters sampled from granitoids: the Vienne Case (France). *Chem. Geol.* 177, 287–308.
- Négrel, P., Petelet-Giraud, E., Barbier, J., Gautier, E., 2003. Surface water–groundwater interactions in an alluvial plain: chemical and isotopic systematics. *J. Hydrol.* 277, 248–267.
- Négrel, P., Petelet-Giraud, E., Widory, D., 2004. Strontium isotope geochemistry of alluvial groundwater: a tracer for groundwater resources characterisation. *Hydrolog. Earth Syst. Sci.* 8 (5), 959–972.
- Parkhurst, D.L., Appelo, C.A.J., 1999. User's guide to PHREEQC (version 2)—a computer program of speciation, batch-reaction, one-dimensional transport, and inverse geochemical calculations: U. S. Geological Survey Water Resource Investigations Report 99-4359, 312 pp.
- Petelet-Giraud, E., Négrel, P., Gourcy, L., Schmidt, C., Schirmer, M., 2007. Geochemical and isotopic constraints on groundwater–surface water interactions in a highly anthropized site. The Wolfen/Bitterfeld megasite (Mulde subcatchment, Germany). *Environ. Pollut.* 148, 707–717.
- Rao, W.B., Chen, J., Yang, J.D., Ji, J.F., Zhang, G.X., 2009. Sr isotopic and elemental characteristics of calcites in the Chinese deserts: implications for eolian Sr transport and seawater Sr evolution. *Geochim. Cosmochim. Acta* 73, 5600–5618.
- Rao, W.B., Chen, J., Tan, H.B., Jiang, S.Y., Sun, J., 2011. Sr–Nd isotopic and REE geochemical constraints on the provenance of fine-grained sands in the Ordos deserts, north-central China. *Geomorphology* 132, 123–138.
- Raiber, M., Webb, J.A., Bennetts, D.A., 2009. Strontium isotopes as tracers to delineate aquifer interactions and the influence of rainfall in the basalt plains of southeastern Australia. *J. Hydrol.* 367, 188–199.
- Roy, S., Gaillardet, J., Allègre, C.J., 1999. Geochemistry of dissolved and suspended loads of the Seine river, France: anthropogenic impact, carbonate and silicate weathering. *Geochim. Cosmochim. Acta* 63, 1277–1292.
- Shand, P., Darbyshire, D.P.F., Love, A.J., Edmunds, W.M., 2009. Sr isotopes in natural waters: Applications to source characterization and water–rock interaction in contrasting landscapes. *Appl. Geochem.* 24, 574–586.
- Su, X.S., Wu, C.Y., Dong, W.H., Hou, G.C., 2011. Strontium isotope evolution mechanism of the Cretaceous groundwater in Ordos Desert Plateau. *J. Chengdu Univ. Technol.* 38 (3), 348–358.
- Venturelli, G., Boschetti, T., Duchi, V., 2003. Na-carbonate waters of extreme composition: possible origin and evolution. *Geochim. J.* 37 (3), 351–366.
- Wang, X.M., Dong, Z.B., Zhang, J.W., Liu, L.C., 2004. Modern dust storms in China: an overview. *J. Arid Environ.* 58, 559–574.
- Wang, Y.X., Guo, Q.H., Su, C.L., Ma, T., 2006. Strontium isotope characterization and major ion geochemistry of karst water flow, Shentou, northern China. *J. Hydrol.* 328, 592–603.
- Woods, T.L., Fullagar, P.D., Spruill, R.K., Sutton, L.C., 2000. Strontium isotopes and major elements as tracers of evolution: example from the upper Castle Hayne aquifer of North Carolina. *Groundwater* 38 (5), 762–771.
- Xie, X.J., Wang, Y.X., Ellis, A., Su, C.L., Li, J.H., Li, M.D., Duan, M.Y., 2013. Delineation of groundwater flow paths using hydrochemical and strontium isotope composition: a case study in high arsenic aquifer systems of the Datong basin, northern China. *J. Hydrol.* 476, 87–96.
- Yang, J.D., Chen, J., An, Z.S., Shields, G., Tao, X.C., Zhu, H.B., Ji, J.F., Chen, Y., 2000. Variations in $^{87}\text{Sr}/^{86}\text{Sr}$ ratios of calcites in Chinese Loess: a proxy for chemical weathering associated with the East Asian summer monsoon. *Palaeogeogr. Palaeoclimatol. Palaeoecol.* 157, 151–159.
- Yang, X.P., Rost, K.T., Lehmkühl, F., Zhu, Z.D., Dodson, J., 2004. The evolution of dry lands in northern China and in the Republic of Mongolia since the Last Glacial Maximum. *Quat. Int.* 118–119, 69–85.
- Yin, L.H., Hou, G.C., Tao, Z.P., Li, Y., 2010. Origin and recharge estimates of groundwater in the Ordos Plateau, People's Republic of China. *Environ. Earth Sci.* 60, 1731–1738.
- Yin, L.H., Hou, G.C., Su, X.S., Wang, D., Dong, J.Q., Hao, Y.H., Wang, X.Y., 2011a. Isotopes (δD and $\delta^{18}\text{O}$) in precipitation, groundwater and surface water in the Ordos Plateau, China: implications with respect to groundwater recharge and circulation. *Hydrogeol. J.* 19, 429–443.
- Yin, L.H., Hu, G.C., Huang, J.T., Wen, D., Dong, G., Wang, J.Q., Li, X.Y., 2011b. Groundwater-recharge estimation in the Ordos Plateau, China: comparison of methods. *Hydrogeol. J.* 19, 1563–1575.
- Zhu, Z., Wu, Z., Liu, S., Di, X., 1980. *An Outline of Chinese Deserts*. Science Press, Beijing, pp. 1–108 (in Chinese).